Author(s):	Auer, Sanna; Koho, Tiia; Uusi-Kerttula, Hanni; Vesikari, Timo; Blazevic, Vesna; Hytönen, Vesa
Title:	Rapid and sensitive detection of norovirus antibodies in human serum with interferometry biosensor
Year:	2015
Journal Title:	Sensors and Actuators B: Chemical
Vol and number:	221
Pages:	507-514
ISSN:	0925-4005
Discipline:	Biochemistry, cell and molecular biology; Medical engineering
School /Other Unit:	BioMediTech; School of Medicine
Item Type:	Journal Article
Language:	en
DOI:	http://dx.doi.org/10.1016/j.snb.2015.06.088
URN:	URN:NBN:fi:uta-201508062215

Rapid and sensitive detection of norovirus antibodies in human serum with a biolayer interferometry biosensor

Sanna Auer[1,3], Tiia Koho[1], Hanni Uusi-Kerttula[2], Timo Vesikari[2], Vesna Blazevic[2] and Vesa P. Hytönen[1,3,*]

[1]BioMediTech and [2]School of Medicine, University of Tampere, Finland

[3]Fimlab Laboratories Ltd., Tampere, Finland

*Please address correspondence to Vesa P. Hytönen, BioMediTech, Biokatu 6, FI-33520 Tampere, Finland. Email: vesa.hytonen@uta.fi

Abstract

Here, we describe the use of a biolayer interferometry biosensor for the fast and sensitive detection of virus-specific antibodies from human serum samples. Norovirus-like particles and norovirus P-particles were used to functionalise the biosensor tip. The detection of antibodies directly from serum samples was challenging, but the addition of a metal chelator (DAB) combined with an anti-human horseradish peroxidase-tagged antibody enabled enhanced detection of virus-specific antibodies in serum dilutions up to 1:100,000. Biolayer interferometry provides results faster than an ELISA, with results in as little as 10-20 minutes when using pre-functionalised sensors. Therefore, biolayer interferometry combined with DAB enhancement offers an attractive method for quick and sensitive quantification of biomolecules from complicated sample matrices.

KEYWORDS: biolayer interferometry, norovirus, virus-like particles (VLPs), P-particles, non-labelled detection, fast diagnostics

1. Introduction

To provide the proper cure and prevent the spreading of diseases, it is important to find the cause of an infection promptly and preferably directly from biological material that has undergone minimal processing. However, the majority of diagnostic samples currently used, such as serum, blood, saliva, stool and urine, are quite difficult to work with. This is partly because these sample specimens are viscous, turbid and contain particles that may cause difficulties when applied to analysers equipped with narrow capillaries. Additionally, coloured sample materials can cause problems if the measurement is based on optical methods. To avoid these challenges, the sensitivity of an assay is often increased by labelling the analyte with tags, such as radionuclides, enzymes or fluorophores. There are also non-labelled measurement technologies available, such as biolayer interferometry (BLI), that are proposed to overcome the above mentioned problems caused by difficult sample matrix.

BLI is a label- and fluidics-free, real-time detection and monitoring system based on light intensity interference [1-4]. Interference changes between the intensities of the reflected light beams are used to measure changes in the molecular layer immobilised on the sensor surface. There are several chemistries available for the biofunctionalisation of the sensors, and we chose Ni-NTA (nickel-charged nitrilotriacetic acid) sensors for this study. While BLI is a label-free measurement system, the measurement signal can be enhanced by the addition of DAB (3,3´-diaminobenzidine) which precipitates after oxidation by horseradish peroxidase (HRP) on the sensor surface [5-7].

Noroviruses (NoV) infect people of all ages and are a major cause of acute epidemic gastroenteritis worldwide. It has been estimated that there are over 20 million annual infections in the United States alone [8]. Symptoms appear 12 – 48 h after viral infection and are characterised by acute onset of nausea, vomiting, abdominal cramps and diarrhoea. Infection can be severe for small children, elderly people and immunocompromised persons, leading to hospitalisation to prevent severe dehydration. The virus is spread by contaminated food and water and from person to person via the faecal-oral pathway and can be further transmitted to food and food contact surfaces by virus-contaminated hands [9-10]. Because the biological characterisation of human NoV has been hampered by the lack of an appropriate cell culture system and animal model for the propagation of the virus, virus-like particles (VLPs) have been used extensively to study NoV

structure and stability, host-cell interactions, and as a tool in diagnostic serological assays [10-13]. Structural studies have shown that the noroviral capsid is composed almost entirely of the 58 kDa VP1 capsid protein [13], which self-assembles into empty capsids called virus-like particles (VLPs) when expressed recombinantly in insect cells or in yeast [14]. In this study, we utilised recently developed His-tagged VLPs (Koho et al., manuscript submitted), which are based on norovirus VLPs described earlier [15]. VLPs are morphologically and antigenically similar to the infectious virion [16]. There are 180 copies of VP1 in a NoV particle, and the diameter of the capsid is approximately 40 nm [16]. VP1 consists of two domains, the shell (S) domain and the protruding (P) domain, and the domains are linked by a short hinge. The P-particles are formed by 12 P-domain dimers, and the diameter of NoV P-particle is approximately 10-15 nm [17].

Recombinant NoV antigens are used in this study to evaluate the potential of the BLI biosensor to detect NoV antibodies from human serum samples. Our results suggest that BLI can be used with clinical samples and it is nearly as sensitive method as ELISA (enzyme-linked immunosorbent assay), but provides results in a much shorter time frame. Due to the BLI measurement set-up (the sensor tip is dipped into the sample matrix) even difficult-to-process bodily fluids (such as saliva, urine, whole blood and stool) can be used as sample materials. We also describe here the successful use of DAB enhancement with serum samples in BLI biosensing. Altogether, our study suggests that BLI combined with DAB enhancement is a highly potent method for rapid and quantitative detection of antibodies in serum samples.

2. Materials and methods

Interferometry biosensing is based on the measurement of white light interference patterns reflected from a reference surface and a biofunctionalised sensor surface. A Fortebio Octet RED384 instrument equipped with 16 parallel biosensors (Fortebio, Pall Life Sciences, Menlo Park, USA) was used in this study. All reagents were of analytical grade.

2.1. NoV-VLP and P-particles

The production and purification of the recombinant P-particles is described by Koho et al. [15] and the His-tagged VLPs will be described in detail by Koho et al. (manuscript submitted). Briefly, a C-

terminal polyhistidine tag was added to the GII-4 NoV capsid protein sequence [15] by polymerase chain reaction using primers that contained the His-tag sequence. The resulting PCR product was cloned under pPH promoter in the baculovirus transfer vector pFastBac^{TM} Dual (Invitrogen, Carlsbad, CA), and the correct sequence was confirmed by DNA sequencing. The recombinant baculoviruses were generated according to the instructions for the Bac-to-Bac Baculovirus Expression System (Invitrogen). The baculoviruses were then used to transfect *Spodoptera frugiperda* insect cells (Sf9; Invitrogen) and the culture was harvested 5-6 days post-infection. The expressed VLPs were purified to homogeneity by Ni-NTA metal ion affinity chromatography by using HisTrap FF Crude column (GE Healthcare, Uppsala, Sweden) with a linear gradient of 20-300 mM imidazole in 20 mM NaH_2PO_4, 500 mM NaCl (pH 7.4). A detailed description of the biochemical and biophysical characterisation of VLPs is given in Koho et al. (manuscript submitted).

2.2. Serum samples

Serum samples from NoV-infected patients were collected as a part of the prospective etiological study at Tampere University Hospital in 2006-2008 [18] and stored at −20°C until they were used. The study protocol was approved by the appropriate Ethics Committee, and informed consent was obtained.

2.3. BLI-measurements

The Ni-NTA sensor surface (Fortebio, Pall Life Sciences, Menlo Park, USA) was functionalised with histidine-tagged NoV-VLPs or NoV P-particles at a concentration of 50 µg/ml in PBS (10 mM $NaPO_3$, 150 mM NaCl, pH 7.4). PBS was used as a liquid phase in all of the BLI sensor functionalisation steps. The immobilisation of the antigens on the sensor surface was completed as follows: 1) the baseline was recorded for 1 minute, 2) NoV-VLPs or NoV P-particles (50 µg/ml in PBS) were immobilised on the sensors for 5 minutes, 3) the sensors were washed in PBS for 2 minutes, and 3) the particles were further amine-coupled with NHS (N-hydroxysuccinimide)–EDC (1-ethyl-3-[3-dimethylaminopropyl]carbodiimide hydrochloride]) treatment for 5 minutes. The amine coupling was performed as described by Johnsson et al. [19], with a freshly made solution

containing 0.025 M NHS and 0.05 M EDC in distilled water. After the NHS-EDC crosslinking step, the sensors were washed in PBS for 2 minutes. 4) Next, to block any remaining unreacted amine-reactive reagents on the sensor surfaces, the sensor was incubated with 1 M ethanolamine-HCl, pH 8.5, for 2 minutes, after which the sensors were washed again for 2 minutes. After this step, the pre-functionalised sensors were stored for 1-2 days in 4°C (immersed in the Octet Kinetics buffer: 10 mM $NaPO_3$, 150 mM NaCl, 0.02% Tween 20, 0.05% sodium azide, 1 mg/ml BSA, pH 7.4).

Typically, the serum analyses were performed using the pre-functionalised sensors within the following 1-2 days. The buffer used in these runs was the Octet Kinetics buffer, as recommended by the manufacturer. First, the baseline was recorded for 1 minute, then the sensors were placed into different dilutions of serum samples for 4 minutes, after which the sensors were washed with the Octet Kinetics buffer for 2 minutes. Next, anti-human IgG labelled with HRP (Vector laboratories Inc., USA, dilution 1:800 in kinetics buffer) was used to detect the NoV antibodies that were bound to the NoV-VLP or NoV P-particle functionalised sensor surfaces. After 5 minutes of incubation, the sensors were washed with Octet Kinetics buffer for 3.5 minutes. Subsequently, the DAB enhancement was performed by dipping the sensors into 0.05% DAB (3,3´-diaminobenzidine)-0.015% H_20_2 in PBS for 5 minutes, after which the sensors were washed in Octet Kinetics buffer for 2.5 minutes. HRP specifically bound on the sensor surfaces oxidise DAB, which precipitates on the sensor surface, causing an enhanced BLI signal.

The temperature of the Octet system was set at 25°C. The stirring speed in all of the measurement phases was 1,000 rpm. Black, tilted-bottom 384-well plates (Fortebio, Pall Life Sciences, Menlo Park, CA) were used as measurement plates to ensure minimal drift in the measured signal between the analysis steps.

BLI data was analysed with the Octet analysis software version 7.1. The initial velocity of the binding reaction was determined by performing a linear regression analysis with Microsoft Excel on the 5-30 sec time window from the beginning of the DAB enhancement step.

2.4. Enzyme-linked immunosorbent assay (ELISA)

ELISAs were used to quantify the NoV antibodies from human serum samples and were performed essentially as described in Koho et al. [15] and Tamminen et al. [20]. Briefly, NoV VLPs and Nov P-

particles were used as coating antigens in enzyme-linked immunosorbent assays (ELISAs) conducted with human sera. All assay wells contained 50 µl. The reagents and test samples were diluted in 1% skimmed milk in phosphate-buffered saline (PBS)/0.05% Tween 20, and the plates were washed with PBS/0.05% Tween 20 between each incubation step. The NoV particles were coated on 96-well high binding microtiter plates (Costar, Corning, NY) at 0.5 µg/ml overnight at 4°C. Serum samples were serially diluted two-fold dilution to obtain a range of 1:100 – 1:102,400 and were added to plates that had been blocked with 5% skimmed milk in PBS for 1 h at 22°C. Any antibodies that bound the NoV particles were then detected with goat anti-human IgG (H+L)-HRP (1:30,000) (Invitrogen, USA) for 1 h at + 37°C, followed by 0.4 mg/ml SIGMAFAST™ OPD substrate (Sigma, Germany) for 15 minutes at + 22°C and 25 µl of 2 M H_2SO_4 to stop the reaction. The optical density (OD) was measured at 490 nm on a Victor^2 1420 Multilabel Counter (Wallac, Perkin Elmer) plate reader. Blank wells were incubated with buffer lacking VLPs and data are expressed as the average OD of duplicate wells from a single experiment.

2.5. SDS-PAGE analysis

The His-tagged NoV VLP and P-particle samples were run on a 12% SDS-PAGE gel and subsequently visualised by Oriole™ Fluorescent Gel Stain (Bio-Rad, Hercules, CA) or Coomassie brilliant blue, respectively.

2.6. Electron microscopy

The primary morphology and size of the NoV VLPs were characterised by examining 3% uranyl acetate-stained samples by transmission electron microscopy (TEM, JEOL JEM-1400).

2.7. Dynamic light scattering

The hydrodynamic diameters of the NoV VLPs and P-particles were calculated as averages of six consecutive measurements, each containing 16 × 10 second readings, performed at 25°C on a Zetasizer Nano ZS dynamic light scattering instrument (Malvern Instruments Ltd., Worcestershire, UK). Predetermined viscosity and refractive index values were also used.

3. Results and discussion

Proper immobilisation and presentation of antigens on the biosensor surface is critical for the sensitive detection of antibodies. Given that a previous study indicated that NoV VLPs are more potent immunogens than P-particles, we were initially interested in comparing the antigenicity of these oligomeric protein complexes [20]. We have recently developed His-tagged NoV VLPs (Koho et al., manuscript submitted), which are comparable to the conventional NoV VLPs described by Koho et al. [15] in terms of their antigenicity. His-tagged NoV VLPs are thus as potent as conventional VLPs and could potentially be a tool for various methods involving the metal-binding characteristics of histidines. Recombinantly expressed VP1 capsid proteins (58 kDa, Fig. 1B) self-assemble into VLPs. Here we utilised recently developed His-tagged VLPs (Fig. 1B) [15]. The NoV particle capsid, which is composed of 180 copies of VP1, has a diameter of 40 nm [17], which we confirmed here with dynamic light scattering and TEM (Fig. 1A and 1C). P-particles (Fig. 1D and 1E) were produced by expressing the recombinant capsid protein fragment corresponding to the P-domain in *E. coli* (Fig. 1F). The orientation of VP1 is similar in P-particles and in VLPs, resulting in similar surface antigenic structures to NoV [17].

Fig.1.

Histidine-tagged NoV-VLPs (referred to hereafter as NoV-VLPs) or NoV P-particles were immobilised on BLI Ni-NTA sensors (Fig. 2A) and used to detect NoV-specific antibodies from human serum samples (Fig. 2B). The workflow of the measurement and the corresponding BLI curves are shown in Fig. 2. After determining the binding response directly from serum samples, anti-human IgG conjugated to HRP was applied on the biosensors. This made it possible to further enhance the binding signal with DAB, a metal chelator.

Fig.2.

The aim of this study was to evaluate whether BLI could be used for fast and reliable detection of an analyte from serum samples. NoV cases are typically diagnosed by real-time RT-PCR (reverse transcriptase polymerase chain reaction) [21] on material from the infective source, such as water, food or stool samples, but diagnosis based on antibodies has largely been used after the acute phase of disease [22]. BLI is a robust technology, and the instrumentation allows the use of heterogeneous and complex sample materials (whole blood, serum, urine and saliva) and is simple

to set up. Therefore, BLI may offer a reasonable alternative to traditional methods in the analysis of clinical samples.

3.1. Norovirus antibody detection directly from the serum

We first assessed the capability of BLI to detect the norovirus antibodies directly from the serum samples. The analysis was performed on 7 NoV positive serum samples. A serum sample from a patient lacking a NoV-specific IgG titre by an ELISA was chosen as a negative control. In this context, it is noteworthy that due to the high incidence of norovirus infection from early infancy, it is difficult to obtain access to completely NoV-negative serum samples. After immobilisation of the NoV VLPs or NoV P-particles on the Ni-NTA sensors, they were covalently cross-linked via NHS-EDC to avoid leakage of the immobilised antigens from the Ni-NTA sensor surface. However, when comparative experiments without crosslinking (Fig. 2B) were performed, we found that crosslinking is not absolutely necessary step and reasonably stable sensors were obtained even without crosslinking. This finding was especially true in the case of VLP, which has more His-tags per particle, resulting in strong avidity. Therefore, if a fast analysis is the main priority, the crosslinking-step could be omitted. However, covalent crosslinking may be essential if one is wished to use pre-functionalised sensors and enable a more sensitive detection due to a better baseline reading. Importantly, if using commercially available stabilised DAB solutions, the sensors may need to be covalently functionalised due to the presence of chelating agents, such as EDTA (ethylene diamine tetra-acetic acid), which chelates the Ni^{2+} ions and thus may strip the His-tagged molecules away from the Ni-NTA sensor surface.

Fig. 3A shows that reliable label-free detection of NoV antibodies directly from serum samples is not possible. There is virtually no difference in the BLI responses measured for the NoV-negative or -positive serum samples (the samples selected based on the ELISAs). We also found no difference between the sensors functionalised with P-particles or NoV VLPs. However, after DAB enhancement, there was a marked increase in the BLI signal (Fig. 3B). The positive serum samples gave clearly detectable signals with serum dilutions up to 1:100,000, while the negative serum showed negligible responses after DAB enhancement (Fig. 3B and 3C).

Fig. 3.

The sensors functionalised with P-particles showed higher background responses compared with VLP-functionalised sensors (Fig. 3A), which was most obvious at higher dilutions (1:10,000 and 1:100,000). The same phenomenon was observed after DAB amplification (Fig. 3C), where negative serum showed a higher signal with the P-particle-functionalised sensor compared with the VLP-functionalised sensor. This could reflect differences in the structural features of the P-particles, which is an artificial assembly of capsid protein fragments and thus may be more prone to cause nonspecific binding.

3.2. Sensitivity and dynamic range of BLI versus ELISA

The sensitivity of the BLI assay with DAB enhancement was next compared to that of an ELISA by analysing two NoV-positive serum samples and one negative serum sample (Fig. 4). We observed essentially no response with the negative serum sample up to a 1:100 dilution when analysed with BLI (Fig. 4B and 4E). The standard deviation between parallel samples was low and therefore, both NoV-positive samples showed a clear difference from the negative sample with dilutions in the range of 1:100 to 1:10,000 in the case of the NoV VLP-functionalised sensor (Fig. 4B). In the case of the P-particle-functionalised sensors, the negative serum had a slightly higher response and therefore serum dilutions in the range of 1:100 to 1:1,000 clearly exhibited a higher signal compared to the negative control (Fig. 4E).

An ELISA indicated saturation of the signal with serum dilutions in the range of 1:100 to 1:1,000 (Fig. 4A and 4D). In contrast, our BLI-based assay enabled sampling of 1:100 diluted samples with a predictable signal (Fig. 4B and 4E), as clearly observed in the log-log plot (Fig. 4C and 4F). Therefore, we can claim that BLI has a broad dynamic range and performs better than an ELISA at low sample dilutions. In practice, this means that a quantitative measurement of antibody concentrations can be performed with the BLI assay with a few or just one dilution of each sample, while a quantitative ELISA would require assaying several samples to avoid signal saturation.

Fig. 4.

3.3. Correlation between an ELISA and the BLI assay

Next, we were eager to determine whether the BLI assay provided results comparable to an ELISA with a larger set of serum samples. Therefore, 7 NoV-positive serum samples and one negative

serum sample were analysed in parallel with both methods. A serum dilution of 1:3,200 was selected as a representative measure of an ELISA signal because it did not cause signal saturation with any of the serum samples. We found relatively good correlation between the results with the P-particle based assay when the BLI response measured with a serum dilution of 1:100 was compared to the ELISA results (R^2=0.81) (Fig. S1). In the case of NoV VLP-particles, the correlation was not as high (R^2=0.60). We observed no significant differences in the correlation between the ELISA and BLI assay when 1:100 and 1:1,000–diluted samples were used in the BLI assay. However, further diluting the samples (to 1:10,000) led to a dramatic drop in the correlation in the P-particle-based assays (Fig. S1), indicating that the most reliable quantification was obtained with BLI conducted on moderately diluted samples.

We then asked whether BLI combined with DAB might be suitable for the quantification of the antibodies. Therefore, the initial velocity of the DAB enhancement reaction was determined from the data. Fig. 5 shows the initial rate plotted against the reciprocal of the dilution factor. Presenting the data in this manner reveals a strong concentration dependent response. Serum2 gave the highest binding rates, while negative serum showed basically no correlation between the initial reaction velocity and the sample concentration. P-particle-functionalised sensors showed higher initial velocities compared to NoV VLP functionalised sensors, which again may reflect the differences in the chemical structure of the antigens. Therefore, we conclude that the initial velocities obtained during the DAB enhancement step can be used as a reliable method to determine the concentration of the analyte. The good correlation between sample concentration and the initial rate of DAB enhancement reaction can be further visualized by plotting the results using a log-log plot (insets in Fig. 5).

Fig. 5.

Another way to evaluate the sensitivity of BLI is to determine the limit of detection (LOD). By using the reading for a negative serum sample, we obtained a LOD as follows: LOD = response of a negative control sample + 3 x standard deviation. The measured responses were then plotted with the determined LODs (Fig. 6). This analysis illustrates that a BLI assay conducted with VLP-functionalised sensors can distinguish between negative and positive samples in all dilutions used (1:100, 1:1,000, 1:10,000), while the P-particle-functionalised sensors performed less reliably; a serum dilution of 1:100 was the only condition that yielded a signal above the LOD for all the NoV-

positive serum samples. Typically, the dilution range in immunoassays in clinical setting is within 1:2 to 1:100 000 [23]. However, this is highly dependent on the analyte of interest, on the stage of the disease as well as on the method used. Therefore, the range of sample dilutions studied here is reasonable concerning clinical applications.

Fig. 6.

There are NoV antibody-based lateral flow tests available for fast diagnosis, and they are used mainly for rapid screening of stool samples [24]. Stool samples are preferred due to the high virus content. Enzyme immunoassays for NoV have also been developed, and the commercial kits available are based on immobilising several different antibodies against various NoV genogroups, as reviewed by Vinje [25]. However, the most accurate and genotype-specific NoV analysis are real-time PCR assays conducted in clinical research laboratories with the required facilities and trained personnel [26]. Norovirus detection has also been performed with aptamers [27], and magnetic beads have been used successfully especially for rising the analyte concentration [28]. However, besides the ELISA and PCR-methods, there are only a few non-labelled measurement technologies available suitable for clinical samples. Surface plasmon resonance (SPR) is non-labelled and very sensitive technique, which has been demonstrated also with serum samples [29], but is not suitable as such for routine clinical analysis with difficult sample matrix and multiple sample specimens. In a recent article by Khare et al. [30], detection of gastro-intestinal pathogen was compared with two analysers based on multiplexed PCR reactions. This analysis revealed that both PCR-based multiplex panels demonstrated high sensitivity and noroviruses were among the most commonly detected pathogens. The BLI assay could also be multiplexed and the analysis time per sample seems to be faster with BLI compared with the multiplexed-PCR assays, where the time per run is 1-3.5 hrs [30].

Our results suggest that BLI could be suitable for rapid diagnostics of viral (and other) infections from various biological samples. For example, this methodology could be implemented at airports for rapid screening of infectious diseases, which has been widely discussed lately due to the recent outbreak of ebolavirus.

4. Conclusions

BLI is a robust technology and could replace ELISA in many situations but especially when rapid quantitative analysis is required. BLI combined with DAB enhancement offers high dynamic range but is slightly less sensitive compared with an ELISA. With pre-functionalised sensors, the method of detecting antibodies from serum samples described here could be performed in 10-20 minutes, which is appealing in situations where rapid decisions are needed. The BLI sensor is straightforward to operate and does not require extensively trained personnel.

Acknowledgements

We acknowledge Academy of Finland (grants 136288, 273192 and 263540) for financial support. We thank Biocenter Finland for infrastructure support. We thank Ulla Kiiskinen and Niklas Kähkönen for excellent technical assistance. The sponsors had no role in study design; in the collection, analysis and interpretation of data; in the writing of the report; and in the decision to submit the article for publication.

References

[1] M.T. Lotze, Label-free, real-time detection system for molecular interaction analysis. US Patent 2009/0147264A1.

[2] Y. Abdiche, D. Malashock, A. Pinkerton, J. Pons, Determining kinetics and affinities of protein interactions using a parallel real-time label-free biosensor, the Octet, Anal. Biochem. 377 (2008) 209-217.

[3] R.L. Rich, D.G. Myszka, Higher-throughput, label-free, real-time molecular interaction analysis, Anal. Biochem. 361 (2007) 1-6.

[4] A.M. Farkas, T.M. Kilgore, M.T. Lotze, Detecting DNA: getting and begetting cancer, Curr. Opin. Invest. Drugs 8 (2007) 981-986.

[5] V.D. Nadkarni, R.J. Linhardt, Enhancement of diaminobenzidine colorimetric signal in immunoblotting, BioTechniques 23 (1997) 382-385.

[6] S.H. Choo, W. Ma, J. Wei, Precipitating substrate for bio-layer interferometry, United States patent application publication. Pub. No.: US 2011/0236911 A1. Pub. Date: Sep. 29, 2011.

[7] Y. Liu, P. Estep, F. Reid, Y. Cao, T. Sun, Y. Yu, I. Caffry, Y. Xu, Picomolar solution phase affinity measurement by BLI-ELISA, Fortebio Interact. Winter 7 (2014) 7-9.

[8] E.F. Donaldson, L.C. Lindesmith, A.D. LoBue, R.S. Baric, Viral shape-shifting: Norovirus evasion of the human immune system, Nat. Rev. Microbiol. 8 (2010) 231-241.

[9] M. Koopmans, E. Duizer, Foodborne viruses: an emerging problem, Int. J. Food Microbiol. 90 (2004) 23-41.

[10] M.M. Patel, A.J. Hall, J. Vinje, U.D. Parashar, Noroviruses: a comprehensive review, J.Clin.Virol. 44 (2009) 1-8.

[11] S.F. Ausar, T.R. Foubert, M.H. Hudson, T.S. Vedvick, C.R. Middaugh, Conformational stability and disassembly of Norwalk virus-like particles. Effect of pH and temperature, J.Biol.Chem. 281 (2006) 19478-19488.

[12] K. Nurminen, V. Blazevic, L. Huhti, S. Räsänen, T. Koho, V.P. Hytönen, T. Vesikari, Prevalence of norovirus GII-4 antibodies in Finnish children, J. Med. Virol. 83 (2011) 525-531.

[13] B.V. Prasad, M.E. Hardy, T. Dokland, J. Bella, M.G. Rossmann, M.K. Estes, X-ray crystallographic structure of the Norwalk virus capsid, Science 286 (1999) 287-290.

[14] J. Tomé-Amat, L. Fleischer, S.A. Parker, C.L. Bardliving, C.A. Batt, C.A., 2014. Secreted production of assembled Norovirus virus-like particles from *Pichia pastoris*. Microb. Cell Fact. 13: 134.

[15] T. Koho, L. Huhti, V. Blazevic, K. Nurminen, S.J. Butcher, P. Laurinmäki, N. Kalkkinen, G. Rönnholm, T. Vesikari, V.P. Hytönen, M.S. Kulomaa, Production and characterization of virus-like particles and the P domain protein of GII.4 norovirus, J. Virol. Methods. 179 (2012) 1-7.

[16] X. Jiang, M. Wang, D.Y. Graham, M.K. Estes, Expression, self-assembly, and antigenicity of the Norwalk virus capsid protein, J. Virol. 66 (1992) 6527-6532.

[17] M. Tan, X. Jian, A subviral nanoparticle for vaccine development against norovirus, rotavirus and influenza virus, Nanomedicine (Lond). 7 (2012) 889-897.

[18] M. Malm, H. Uusi-Kerttula, T. Vesikari, V. Blazevic, High serum levels of norovirus genotype-specific blocking antibodies correlate with protection from infection in children, J. Infect. Dis. 210 (2014) 1755-1762.

[19] B. Johnsson, S. Löfås, G. Lindquist, Immobilization of proteins to carboxymethyldextran-modified gold surface for biospecific interaction analysis in surface plasmon resonance sensors, Anal. Biochem. 198 (1991) 268–277.

[20] K. Tamminen, L. Huhti, T. Koho, S. Lappalainen, V.P. Hytönen, T. Vesikari, V. Blazevic, A comparison of immunogenicity of norovirus GII-4 virus-like particles and P-particles, Immunology 135 (2012) 89-99.

[21] A.A. Trujillo, K.A. McCaustland, D.P. Zheng, L.A. Hadley, G. Vaughn, S.M. Adams, T. Ando, R.I. Glass, S.S. Monroe, Use of TaqMan real-time reverse transcription-PCR for rapid detection, quantification, and typing of norovirus, J. Clin. Microbiol. 44 (2006) 1405-1412.

[22] R.I. Glass, U.D. Parashar, M.K. Estes, Norovirus gastroenteritis, N. Engl. J. Med. 361 (2009) 1776-1785.

[23] J.F.M. Jacobs, R.G. van der Molen, X. Bossuyt, J. Damoiseaux, Antigen excess in modern immunoassays: To anticipate the unexpected, Autoimmunity Rev. 14 (2015) 160-167.

[24] G. Geginat, D. Kaiser, S. Schrempf, Evaluation of third-generation ELISA and a rapid immunochromatographic assay for the detection of norovirus infection in fecal samples from inpatients of a German tertiary care hospital, Eur. J. Clin. Microbiol. Infect. Dis. 31 (2012) 733-737.

[25] J. Vinje, Advances in laboratory methods for detection and typing of norovirus. J. Clin. Microbiol. 53 (2015) 373-381.

[26] K.J. Rolfe, S. Parmar, D. Mururi, T.G. Wreghitt, H. Jalal, H. Zhang, M.D. Curran, An internally controlled, one-step, real time RT-PCR assay for norovirus detection and genogrouping, J. Clin. Virol. 39 (2007) 318-321.

[27] A. Giamberardino, M. Labib, E.M. Hassan, J.A. Tetro, S. Springthorpe, S.A. Sattar, M.V. Berezovski, M.C. DeRosa, Ultrasensitive norovirus detection using DNA aptasensor technology, Plos ONE 8 (2013) e79087.

[28] K. Lee, K. Park, D.J. Seo, M.H. Lee, J.-Y. Jung, G.J. Park, D. Yoon, K.H. Park, C. Choi, Enhanced immunomagnetic separation for the detection of norovirus using the polyclonal antibody produced with human norovirus GII.4-like particles, Food Sci. Biotechnol. 23 (2014) 1569-1576.

[29] S. Auer, M. Nirschl, M. Schreiter, I. Vikholm-Lundin, Detection of DNA hybridisation in a diluted serum matrix by surface plasmon resonance and film bulk acoustic resonators. Anal. Bioanal. Chem. 400 (2011) 1387-1396.

[30] R. Khare, M.J. Espy, E. Cebelinski, D. Boxrud, L.M. Sloan, S.C. Cunningham, B.S. Pritt, R. Patel, M.J. Binnicker, Comparative evaluation of two commercial multiplex panels for detection of gastrointestinal pathogens by use of clinical stool specimens, J. Clin. Microbiol. 52 (2014) 3667-3673.

Figure captions

Fig. 1. Antigens used in the biofunctionalisation of the BLI sensor. a) Transmission electron microscopy image of a negatively stained His-tagged NoV VLP. b) SDS-PAGE showing the 58 kDa VP1 capsid protein corresponding to the NoV VLP shown in (a). c) Dynamic light scattering analysis of the NoV VLP sample showing the size distribution of the particles (average diameter ~40 nm). d) Transmission electron microscopy image of negatively stained NoV P-particles. Three individual particles are indicated by arrowheads. Figure (d) is partially adapted from Tamminen et al., 2012 and is used with permission from the publisher. e) SDS-PAGE analysis showing the 35 kDa protein fragment corresponding to the P-domain of the NoV capsid protein. f) Dynamic light scattering of the NoV P-particles showing the size distribution of the particles (average diameter ~15 nm).

Fig. 2. a) Schematic representation of the BLI detection principle utilising NoV-VLP or NoV P-particles as immobilised antigens. The molecular events taking place on the sensor head are shown. In the first stage, the Ni-NTA sensors were functionalised either with His-tagged P-particles or with NoV-VLPs. During the second stage, the NoV antibodies in the serum samples were bound onto the sensor surfaces. Finally, the signal was enhanced in the third stage with DAB, which is oxidised by HRP (horse radish peroxidase)–conjugated anti-human antibodies to form a metal precipitate on the sensor surface. b) An example BLI sensorgrams corresponding to a NoV-positive serum sample. Note that this measurement does not involve covalent coupling of the antigen, which is reflected by the "leakage" of the P-particle from the sensor surface. The red curve corresponds to the NoV P-particle-functionalised sensor and the dashed blue curve to the NoV-VLP-functionalised sensor.

Fig. 3. Detection of NoV antibodies from serum with BLI. a) BLI responses with NoV-negative (open symbols) and NoV-positive (filled symbols) serum samples with sensors functionalised with NoV VLPs (▲) or with P-particles (●). b) BLI responses after the DAB enhancement with the same sensors and samples. c) The data presented in (b) graphed on a logarithmic Y-axis. The values represent the maximum BLI sensor response after a 4 (a) or 5 (b-c) minutes incubation, prior to sensor washing.

Fig. 4. Comparison of the BLI assay and ELISA for detection of NoV antibodies from human serum samples using a-c) NoV VLP as an antigen or d-f) P-particle as an antigen. The filled triangle (▲) and filled circle (●) symbols represent the NoV positive samples, while dash-marks (–) represent the NoV negative sample. a,d) The ELISA responses. b,e) The BLI responses on a linear-logarithmic scale. c,f) The BLI responses plotted on a logarithmic y-axis. The BLI values depicted represent the BLI signal after a 5 minutes incubation in the DAB solution.

Fig. 5. Initial velocities obtained from the DAB-enhancement phase velocity plotted against the reciprocal of the dilution factor. The sensors were functionalised with NoV VLPs (a) or with NoV P-particles (b). The values obtained with Serum2 (Δ), Serum1 (○) and Serum0 (●) samples are shown. The insets depict the same data plotted on a logarithmic scale. The R^2 values are shown next to each curve. The standard deviations are also shown, but were typically so small (less than 5%) that they are obscured by the symbols.

Fig. 6. BLI and ELISA responses for 7 positive and one negative (marked with Δ) serum samples at different dilutions. The LOD value determined for the BLI measurements is marked with a dash (**–**).

Figure 1

Click here to download high resolution image

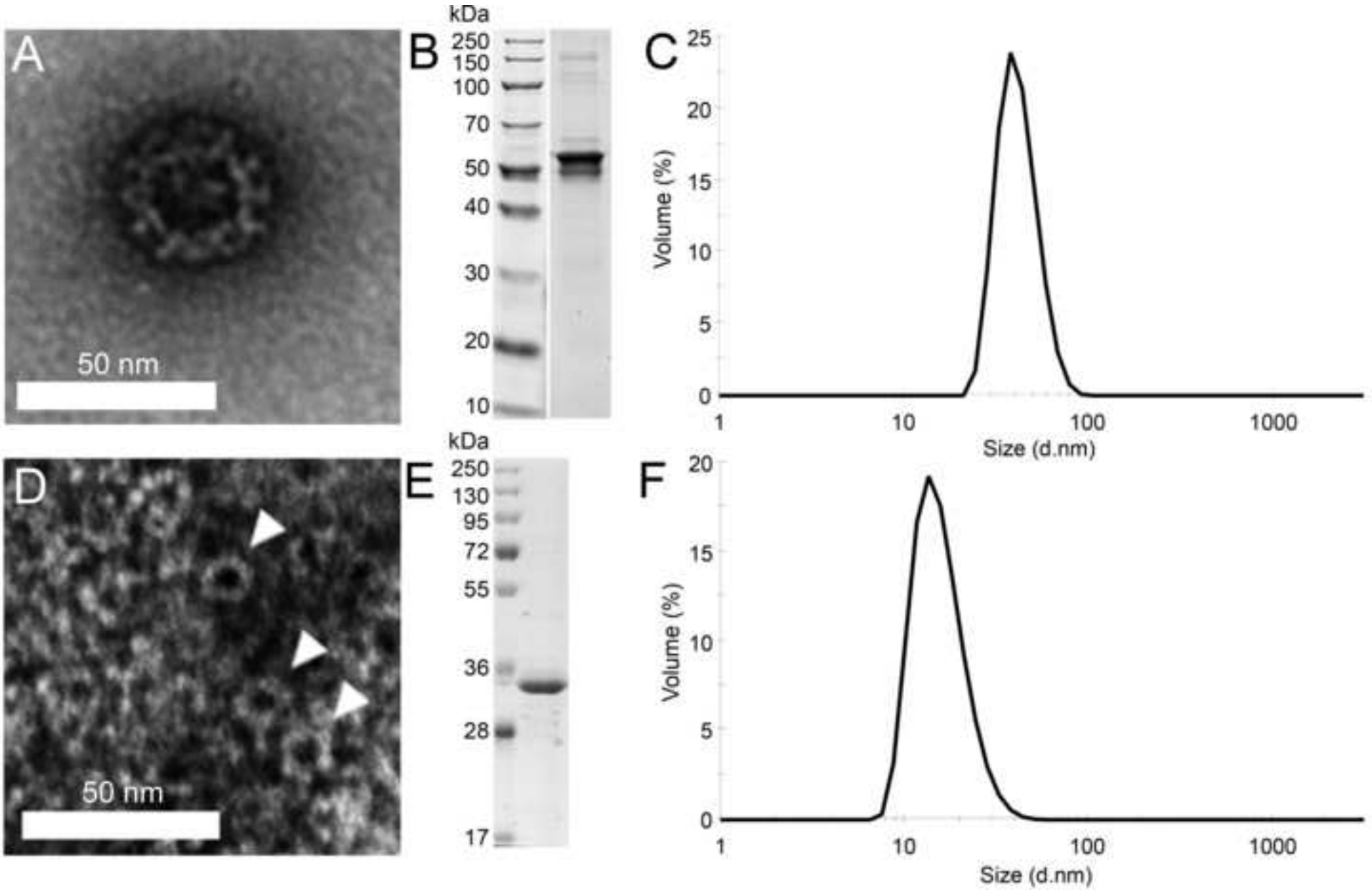

Figure 2

Click here to download high resolution image

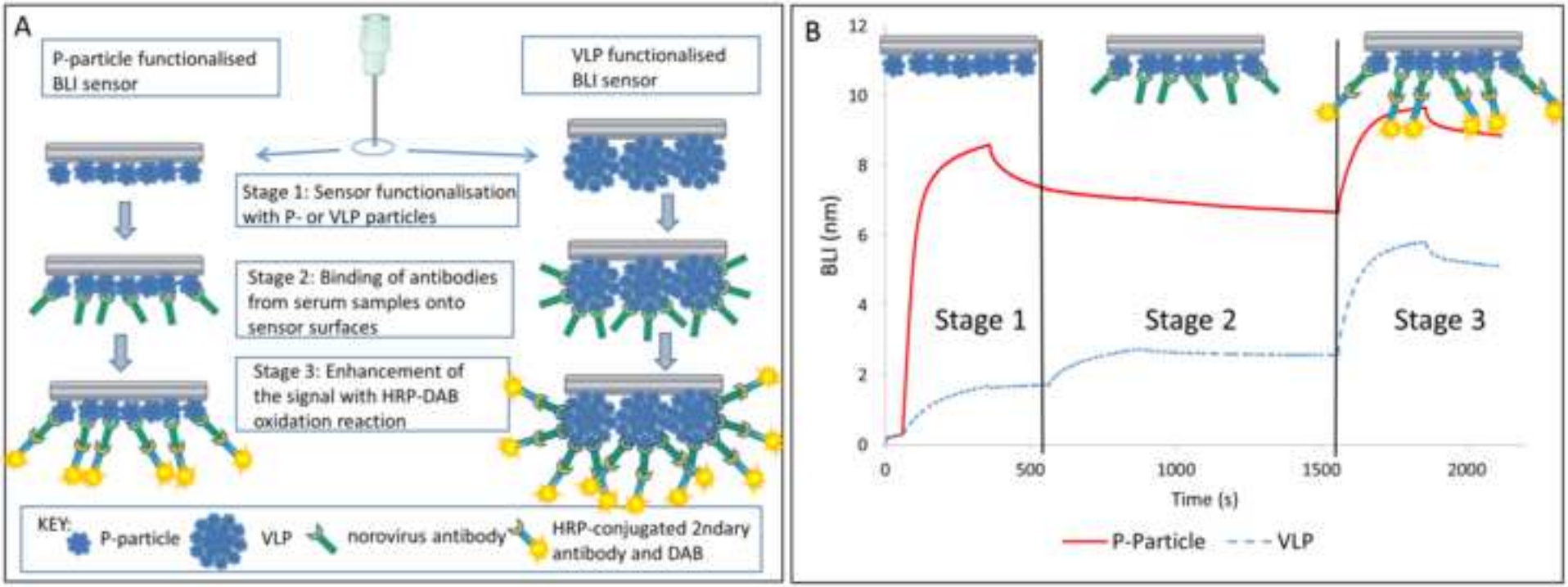

Figure 2-Gray

Click here to download high resolution image

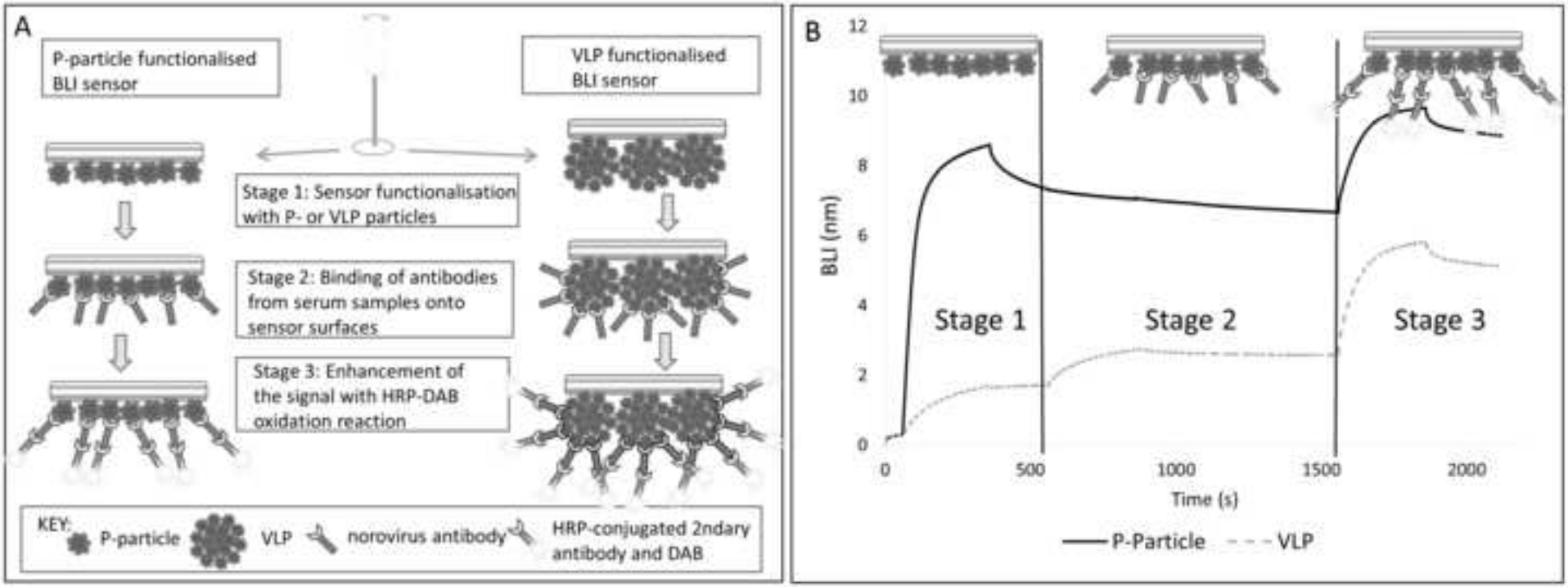

Figure 3

Click here to download high resolution image

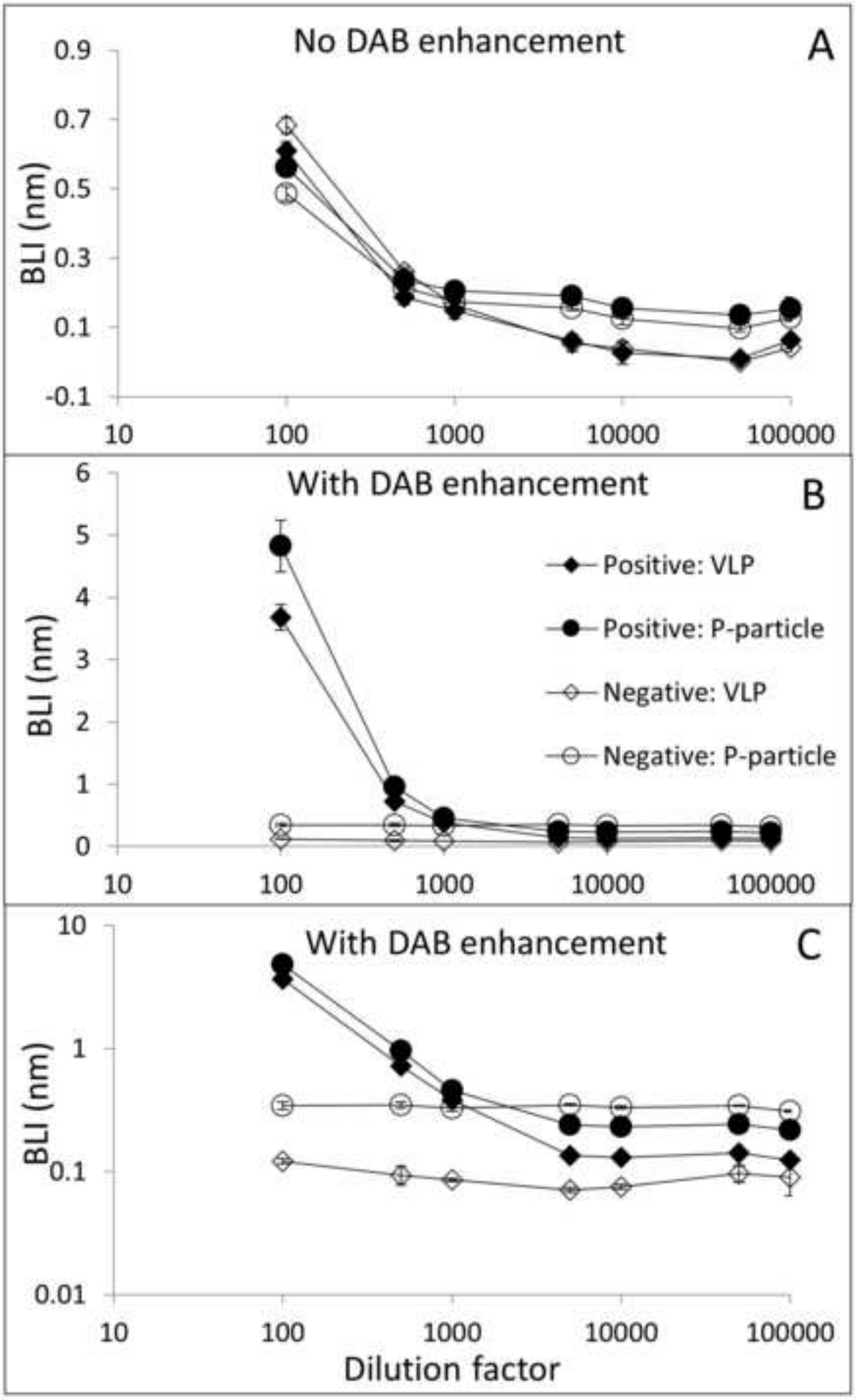

Figure 4

Click here to download high resolution image

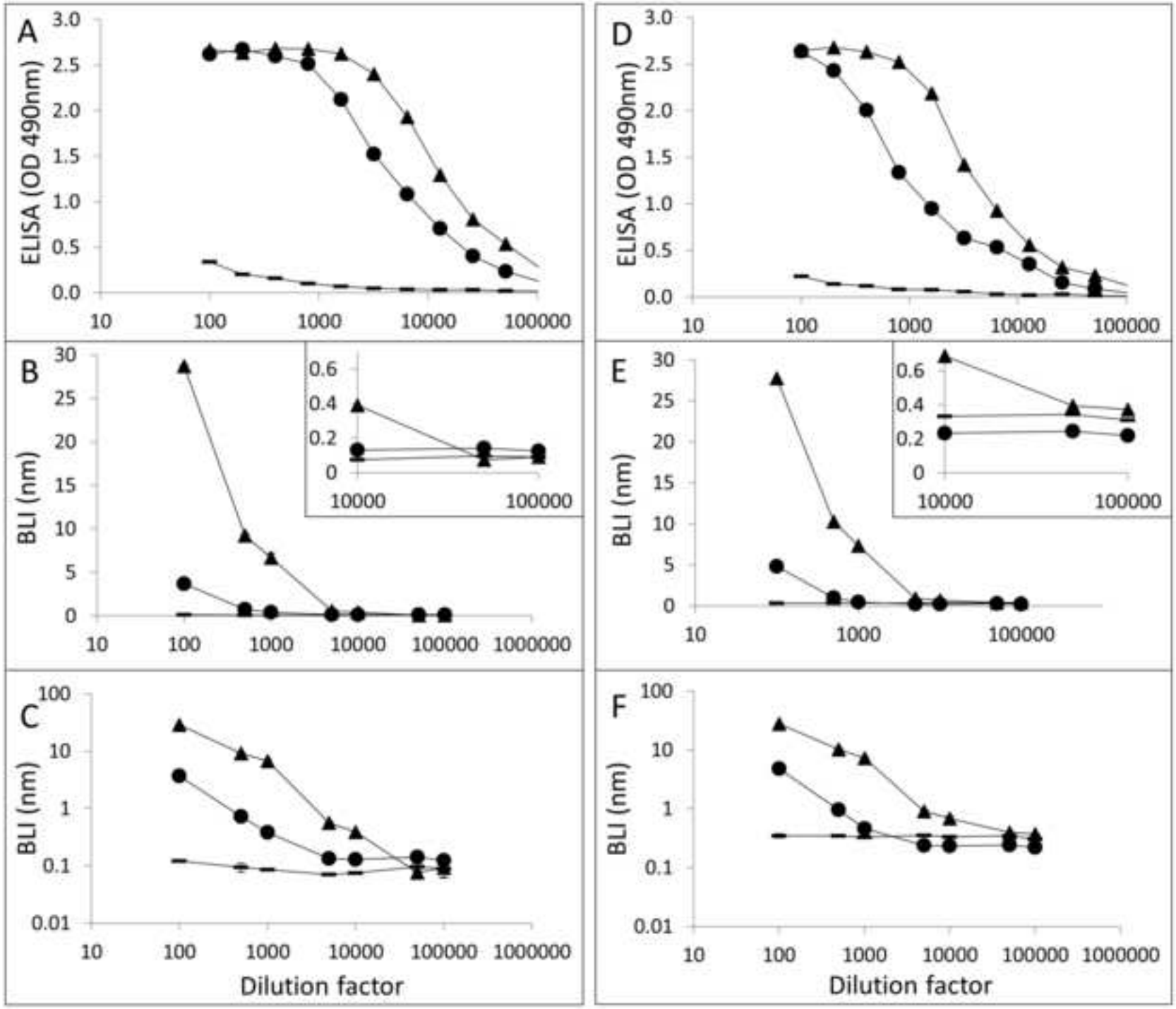

Figure 5

Click here to download high resolution image

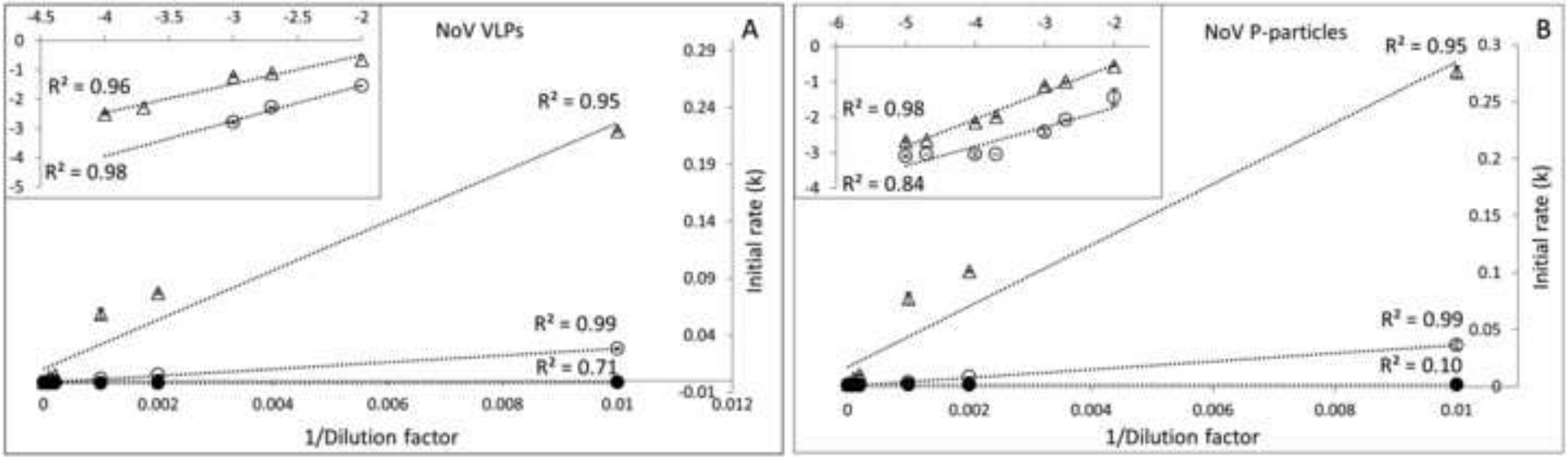

Figure 6

Click here to download high resolution image

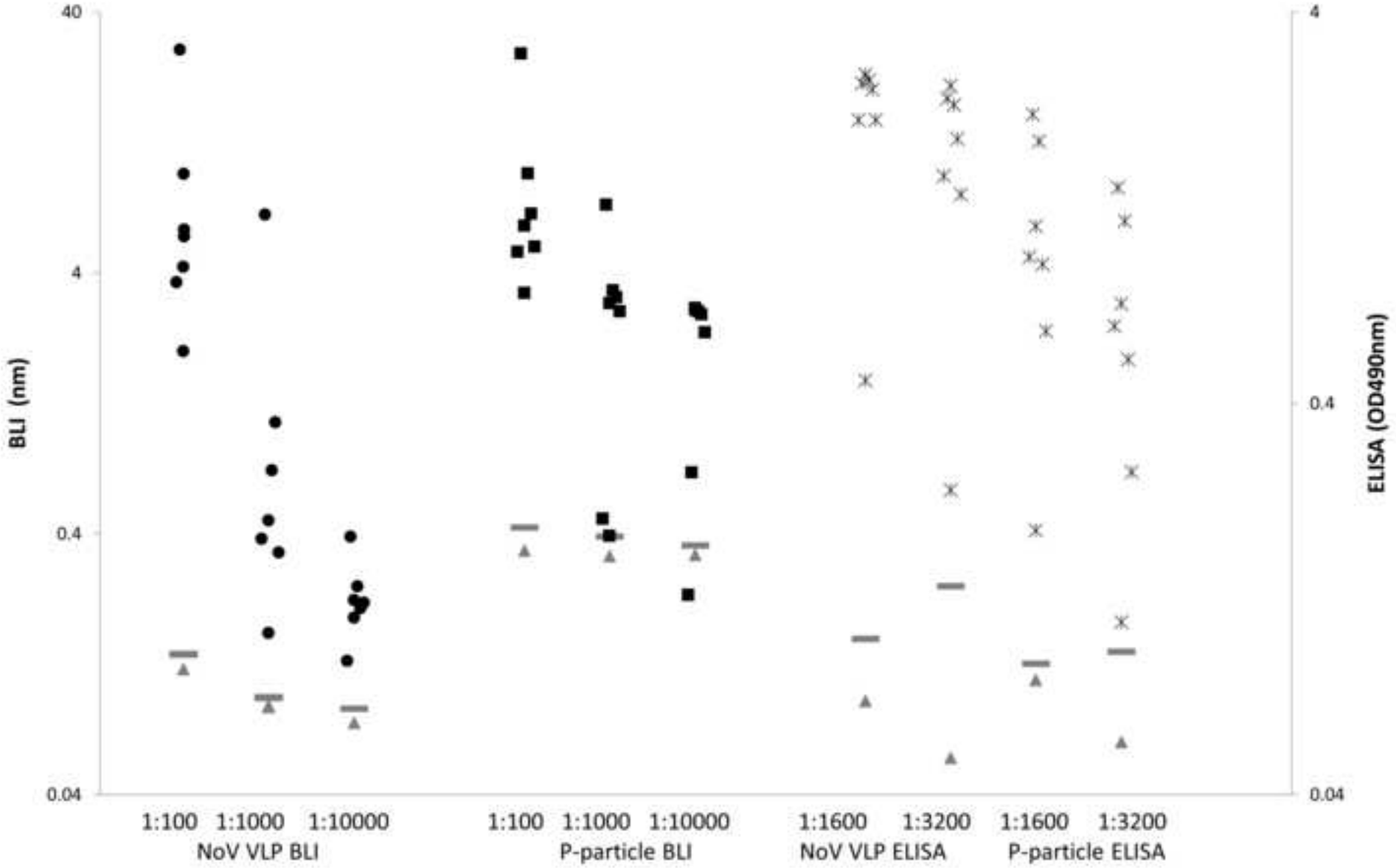

Supplementary Material

Click here to download Supplementary Material: Supplementary material.doc